



OPEN

## Large morphological transitions underlie exceptional shape diversification in an adaptive radiation

Katherine B. Starr<sup>1</sup>, Emma Sherratt<sup>2</sup> & Thomas J. Sanger<sup>1</sup>✉

Adaptive radiations are characterized by an increase in species and/or phenotypic diversity as organisms fill open ecological niches. Often, the putative adaptive radiation has been studied without explicit comparison to the patterns and rates of evolution of closely related clades, leaving open the question whether notable changes in evolutionary process indeed occurred at the origin of the group. *Anolis* lizards are an oft-used model for investigating the tempo and mode of adaptive radiations.

Most of the prior research on the diversification of *Anolis* morphology has focused on the post-cranium because of its significance towards subdivision of the arboreal habitat. But the remarkable diversity in head shape in anoles has not been as thoroughly investigated. It remains unknown whether the tempo or mode of head shape diversification changed as anoles diversified. We performed geometric morphometric analysis of skull shape across a sample of 12 Iguanian families (110 species), including anoles. *Anolis* lizards occupy a unique area and a wider region of morphological space compared to the 11 other families examined. We did not find a difference in the evolutionary rate of head shape diversification between anoles and their relatives. Rather, the extraordinary amount of skull diversity arose through a distinct mode of evolution; anoles moved into novel regions by relatively large morphological transitions across morphological space compared to their relatives. Our results demonstrate that traits not directly tied to the adaptive shift of a lineage into unique ecological spaces may undergo exceptional patterns of change as the clade diversifies.

**Keywords** Skull evolution, Geometric morphometrics, Comparative methods, Macroevolution, Tempo and mode, *Anolis*

Adaptive radiations, when organisms diversify into open ecological niches, are characterized by an increase in the number of species and/or an increase in morphological diversity correlated with the environment in which those species reside<sup>1,2</sup>. Adaptive radiations may be associated with “early bursts” of species number or morphological diversity, although an increase in the rate of diversification is not a requisite parameter of adaptive radiations<sup>1</sup>. Classic examples of adaptive radiation include Darwin’s finches<sup>3</sup>, Hawaiian silverswords<sup>4</sup>, and cichlid fishes<sup>5</sup>. These radiations have been widely studied throughout a range of biological disciplines<sup>6–10</sup>. In many cases the group of interest, the one proposed to have undergone an adaptive radiation, is studied without explicit comparison to the patterns and rates of evolution in a wide sample of closely related clades<sup>11–16</sup>. A comparison between the putative adaptive radiation and its close relatives is vital to understand whether there were changes in the rate or pattern of evolution at the presumed origin of the adaptive diversification<sup>14</sup>.

Morphological traits that directly impact an organism’s ability to take advantage of a unique niche are likely to diverge among species<sup>2,17</sup>. This often occurs in the form of quantitative changes in proportion, such as the case for changes in beak shape among Darwin’s finches<sup>18</sup> or the shape of cichlid fish jaws<sup>19</sup>. Adaptive diversification may also be “triggered” by the evolution of a key innovation, such as floral nectar spurs in angiosperms, the mammalian hypocone, or adhesive toe pads of *Anolis* lizards<sup>11,20–25</sup>. Although those key innovations may be a primary facilitator of adaptive change, the entire organism must continue to function as an integrated whole. Because different parts of the body may diversify to different degrees and at distinct rates of evolution<sup>26,27</sup>, greater attention should be given to all the traits that allow organisms to thrive in different ecological spaces, not just the most obvious traits underlying the transition into novel ecological niches<sup>25</sup>.

<sup>1</sup>Department of Biology, Loyola University Chicago, 1032 W. Sheridan Rd., Chicago, IL 60660, USA. <sup>2</sup>School of Biological Sciences, University of Adelaide, Adelaide, SA 5005, Australia. ✉email: tsanger@luc.edu

*Anolis*, a genus of iguanid lizard, is a widely accepted and well-studied example of an adaptive radiation<sup>16,22,28</sup>. Following the evolution of adhesive toepads this group radiated throughout arboreal niches on the islands of the Caribbean and Central America<sup>11,15,22–24</sup>. After the transition into arboreality, changes in body proportion (e.g., toe pad dimensions, limb length, tail length) allowed anoles to subdivide the arboreal habitat unlike any of their relatives had before. This niche specialization and subdivision lead to extensive speciation, resulting in over 400 extant species in the genus<sup>22</sup>. The diverse postcranial morphologies of anoles, and their large species numbers are classically cited points of evidence showing that this group is a powerful example of an adaptive radiation<sup>2,22</sup>.

The Iguanian relatives of anoles diverged from their squamate ancestors 100–160 million years ago<sup>29</sup>, while the genus *Anolis* diverged approximately 50 million years ago<sup>15</sup>. Fossil evidence suggests the ecomorphological diversity of *Anolis* was present by 15 mya<sup>30</sup>. Iguanian families exhibit a range of species diversity, from fewer than 20 species in Opluridae, Polychrotidae, Leiosaurinae, and Corytophanidae to more than 100 species in Phrynosomatidae and Liolaemidae<sup>31</sup>. With a rich diversity of 289 species<sup>32</sup>, the South American genus *Liolaemus* is also characterized as an adaptive radiation<sup>33,34</sup>. Except for *Anolis* (family Dactyloidae), most Iguanian relatives reside on the ground, and none possess known innovations like toepads<sup>11</sup>. The diversity of relative Iguanian families makes for a great context against which the evolutionary patterns of anoles can be compared.

Research on *Anolis* lizards has focused on the relationship between the postcranial traits involved with locomotion and the structural habitat<sup>17,22,36</sup>. Despite significant diversity in head and skull shape and evidence of ecomorphological signal [Fig. 1, <sup>35,37,38</sup>], the rate and pattern of head shape evolution has not been widely investigated. Herein, we investigate whether: (1) the rate or pattern of evolution of *Anolis* skull diversification is distinct from that of their relatives and (2) anoles exhibit same, similar, or different patterns of morphological variation, compared to that of their relatives. We hypothesized that the adaptive radiation of *Anolis* lizards rapidly generated increased morphological diversity in head shape as these species radiated in the new arboreal niche space.

## Results

We examined skull shape diversity among 110 species representing 12 families of Iguanian lizards, including Dactyloidae (comprised of a single genus, *Anolis*), using geometric morphometrics. Species of the genus *Anolis* were compared to species from the rest of the tree (“their relatives”), and these two groups are referred to as such throughout. All analyses accounted for phylogeny and uncertainty in species relationships using 1000 posterior trees pruned to the focal taxa based upon Tonini et al.<sup>39</sup>.

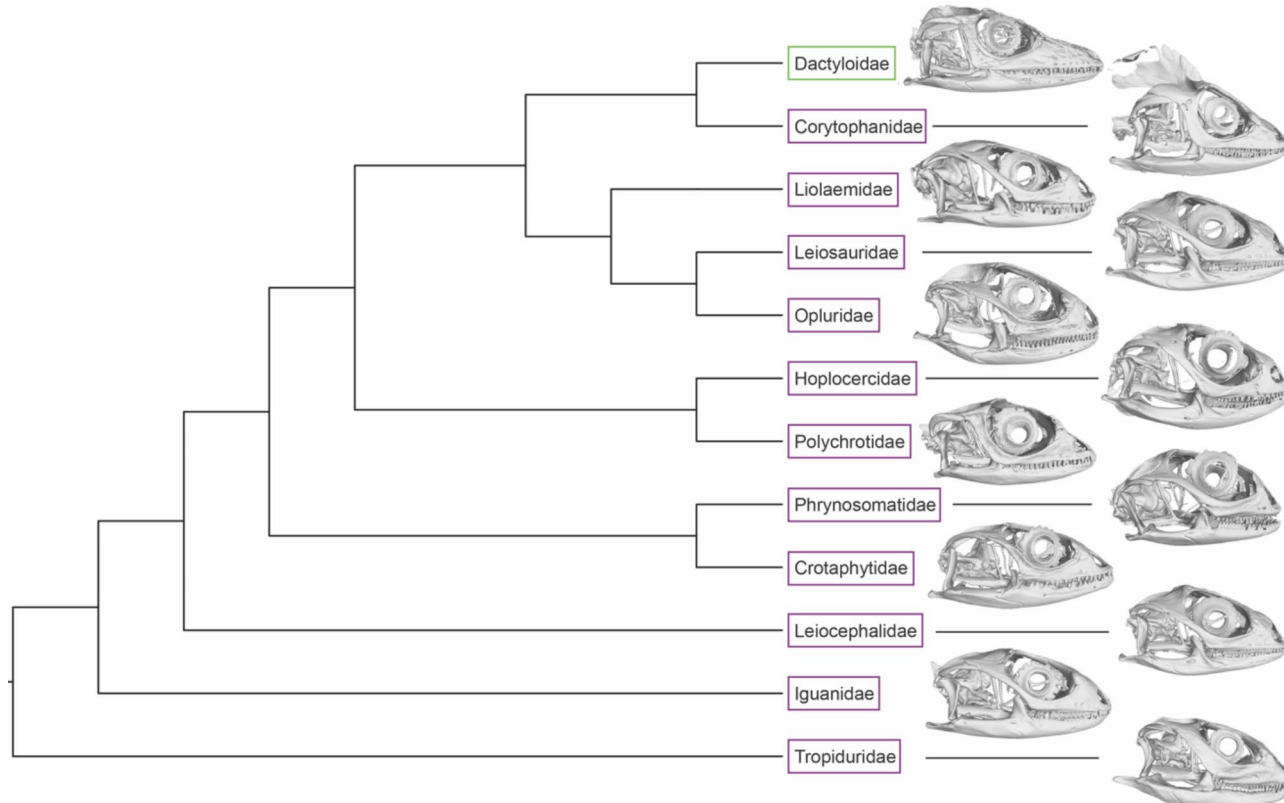


**Fig. 1.** Phylogeny of all Iguania families included in the study with a lateral view skull representative for each. Dactyloidae, indicated by a green box, is comprised of a single genus, *Anolis*, with over 400 recognized species. 11 relative families of *Anolis* are indicated with purple boxes. Topology based on Tonini et al.<sup>60</sup>.

### Iguanian lizard skull diversity

Anoles and their relatives occupy distinct, non-overlapping areas of morphospace along principal component (PC) 1, which represents the degree of cranial elongation (Figs. 2 and 3, Fig. S2). The main axis of variation (PC1, 53.1%) contrasts an elongate-faced narrow cranium (anoles) with a wide, short-faced shape of the relatives (Fig. 3, Fig. S3). Following that, PC2, which accounts for much less of the variation (10.3%), is correlated with changes to the back of the cranium, specifically the width of the posterior region and a change in the shape of the parietals. PC3 and PC4 account for only 6.23% and 4.98% of the variation respectively and were difficult to biologically interpret (Fig. S2).

Evolutionary allometry accounts for 3% of the shape variation among all species (phylogenetic generalized least squares [PGLS] from 1000 trees: median  $R^2 = 0.0344$ , 99.6% of trees with P-value below 0.05). Of the PGLS,

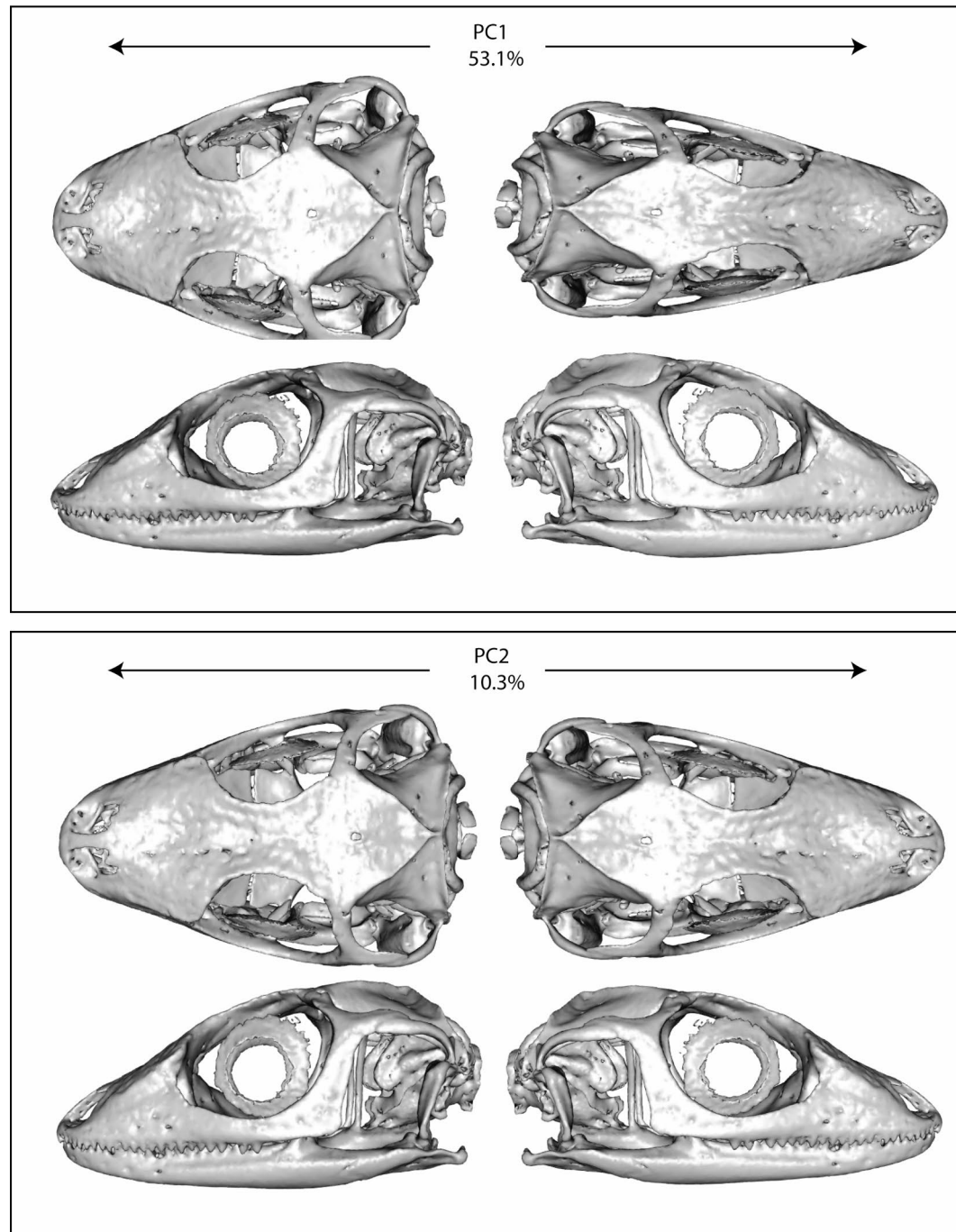


**Fig. 2.** Meshes of the mean skull shape for all specimens were warped to the extreme shape of both principal component (PC) 1 and 2. Minimum values (left) for PC1 are represented by a short-faced, wide skull, while maximum values (right) are represented by a long-faced, narrow skull. PC2 is broadly a difference in skull height, with minimum values (left) with a shorter skull than maximum values (right).

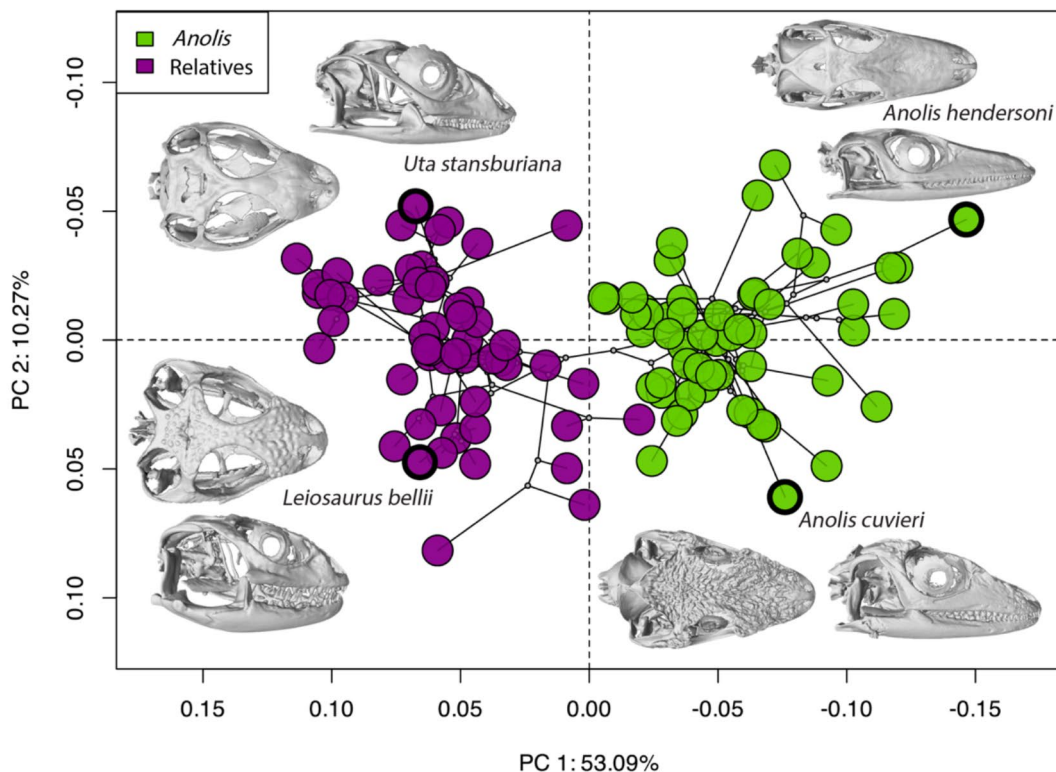


**Fig. 3.** Phylomorphospace represented by principal component (PC) 1 and 2. Skull models for two relative and two anole species have been included to show the difference in skull shape. Relative species have a much shorter face and a wider and taller skull, while anoles have an elongated face with a narrower and flatter skull. Shape changes associated with each axis are visualized in Fig. 2. Node representing the estimated ancestor of *Anolis* is positioned to the right of the origin (0,0).

group factor was significant and the interaction term of cranium size and group was not significant, indicating that *Anolis* and their relatives have distinct but parallel allometric trajectories. Visualizing the relationship with a multivariate regression shows the two groups are distributed along parallel allometric trajectories with different intercepts, where anoles are generally smaller than their relatives (Fig. S1).

#### Disparity and evolutionary rates

We next examined whether anoles and their relatives occupy similar volumes of morphospace (i.e., disparity) by calculating the Procrustes variance (PV) of each group<sup>40</sup>, using the first four principal components, which together account for just under 74.9% of the variance. We found that *Anolis* lizards, members of a single genus, occupy more than two times the volume of morphological space as all 11 closely-related families combined (Fig. 4a; median PV<sub>anolis</sub> = 0.012, median PV<sub>relative</sub> = 0.0055, median P = 0.0009, all 1000 trees significant at 5% level).

To test whether the expansive diversity in head shape was the result of an increased rate of evolution associated with the radiation of anoles, we compared the evolutionary rates of skull shape variation between anoles and their relatives. We found no significant change in the rate of evolution between anoles and their relatives (Fig. 4b;  $s^2_{\text{anolis}} = 6.79 \times 10^{-7}$ ,  $s^2_{\text{relative}} = 7.31 \times 10^{-7}$ , 98.4% of trees with P-value above 0.05).

We estimated disparity through time for skull shape of all 110 species. Disparity relative to the number of species gradually decreases over relative time, from the divergence of Iguanian lizards from the relatives 100–160 million years ago<sup>29</sup> through the point of *Anolis*' divergence at 50 million years ago<sup>15</sup>, and the group's subsequent radiation (Fig. 4d). During the window of relative time estimates corresponding to *Anolis* divergence there are clear fluctuations in disparity but no substantial inflection that would represent a marked increase in disparity with the diversification of the anole radiation. The 95% confidence interval of observed disparity values

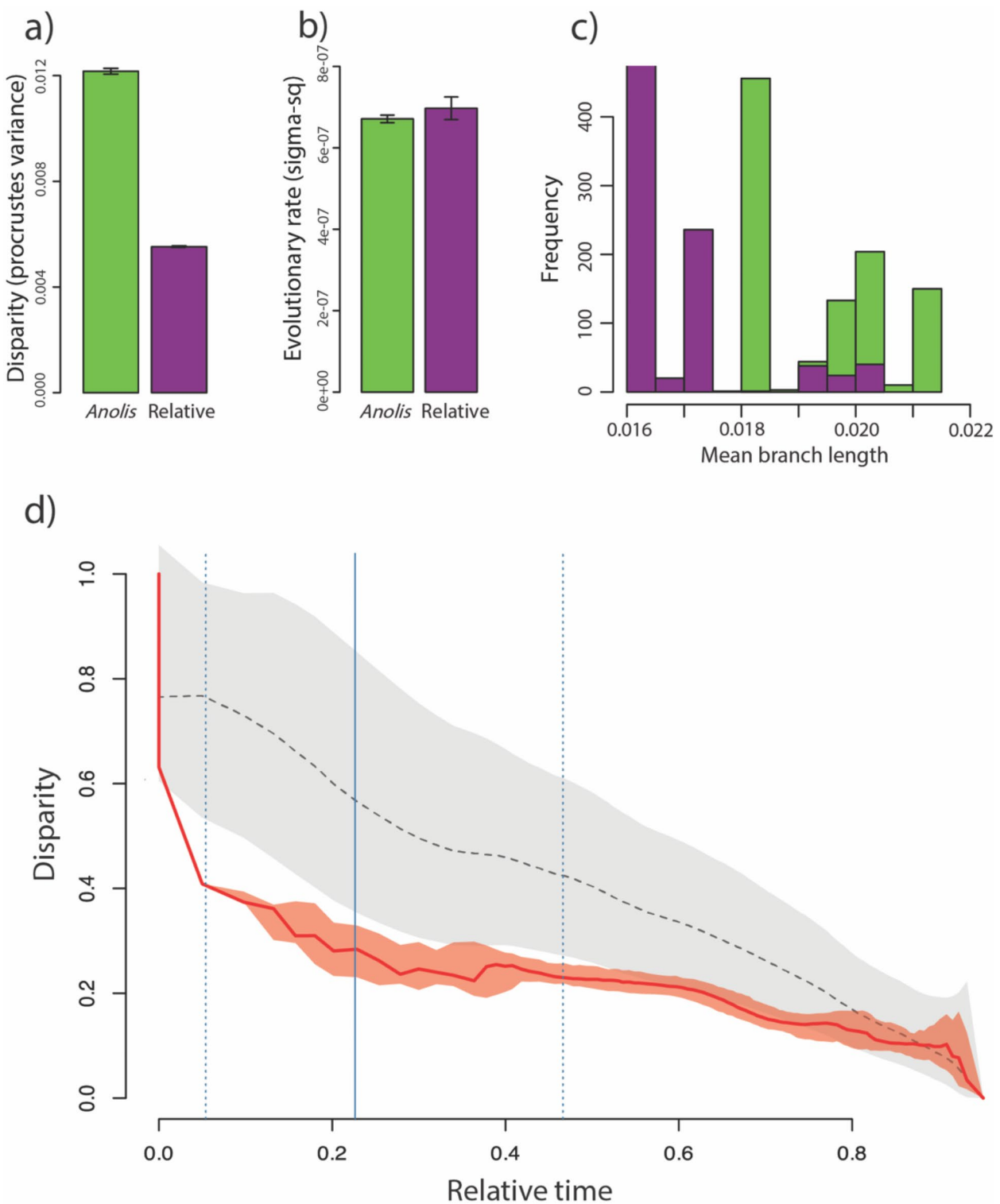


**Fig. 4.** (a) Bar plot of morphological disparity within *Anolis* and their relatives, which is significantly different between the two groups, with anoles exhibiting more than two times more disparity in skull shape than 12 relative families combined. (b) Bar plot of the rate of evolution of skull diversity between anoles and their relatives, which is not significantly different between the two groups. (c) Histogram of the mean branch length for 1000 trees, showing *Anolis*, in green overlaid on their relatives, in purple. Anoles exhibit significantly longer branch lengths. (d) Line plot showing how disparity is changing over relative time. Red represents the observed disparity for all 1000 trees (with 95% confidence interval shaded). Relative age of the *Anolis* clade from the 1000 trees are shown with vertical blue lines (min, median and max). Dotted line represents the median (with 95% confidence interval as grey shaded) of 100 Brownian motion simulations per tree.

remains below the simulated 95% confidence interval of Brownian motion values until relatively recent times (Fig. 4d).

### The mode of evolution

To further interrogate how *Anolis* evolved such widespread skull shape diversity, we investigated the distribution of species in phylomorphospace. First the length of morphometric branches were calculated as the Euclidean distance between nodes or terminal bracketing the branch, which informs us about how much morphological change happened between species<sup>41</sup>. High values indicate a lot of morphological change happened as species diverged from the most recent common ancestor, while shorter morphometric branch length indicates that the change in shape is more conserved, occurring over more gradual, smaller steps. This analysis found that *Anolis* exhibits on average significantly longer branch lengths than the 11 most closely-related families (Fig. 4c; mean branch length<sub>anolis</sub> = 0.0194, mean branch length<sub>relative</sub> = 0.0169, Student's t-test of 1000 trees:  $t=50.304$ ,  $df=1980.5$ ,  $p\text{-value} < 2.2e^{-16}$ ). The range of branch lengths within each group were similar (Fig. S4).

To calculate how densely anoles and their relatives fill their respective morphospaces, we calculated the ratio of the total branch length to the disparity of each group<sup>41</sup>. This analysis revealed that *Anolis* have significantly greater lineage density (LD) than its relatives (Fig. S5; mean LD<sub>anolis</sub> = 1.1404, mean LD<sub>relative</sub> = 1.0361, Student's t-test of 1000 trees:  $t=145.94$ ,  $df=1981.3$ ,  $P\text{-value} < 2.2e^{-16}$ ). Mean ratio (LD<sub>anole</sub>/LD<sub>relative</sub>) of lineage density is 1.096, and for all trees the ratio was greater than 1, indicating that *Anolis* is more effective at diversifying<sup>41</sup>. Taken together, these two analyses demonstrate that *Anolis* diversified in cranial morphology through significantly different modes of evolution than their closely-related Iguanian relatives.

### Discussion

Clades that have experienced an adaptive radiation are often of great interest because of their extensive morphological diversity and/or high number of species<sup>1,2</sup>. However, there remains a lack of understanding of how ecologically important traits, specifically traits that are not key innovations, evolve compared to that of their relatives. Even in some of the most well-studied adaptive radiations, important aspects of morphology are often understudied because they are not perceived to directly correlate with the adaptive diversification of the clade. However, we should likely expect many more organismal features of species to be impacted as they radiate into unique ecological spaces<sup>25</sup>. Here we demonstrate that a trait outside the scope of a key innovation, or one known to be involved with ecological partitioning, diversified extensively into a novel region of morphological space after *Anolis* moved into the arboreal habitat. Our results demonstrate that as anoles shifted into the arboreal habitat, their heads became more elongate and narrower than most of the other Iguanian species in our sample.

The estimated ancestor of *Anolis*, the hypothetical species present at the phylogenetic node where the genus *Anolis* originated, likely evolved on the edge of the cranial morphospace occupied by their relatives. This position is also close to the only other arboreal group in our sampling, the genus *Polychrus* (Fig. S6). Convergence of *Polychrus* and *Anolis* in morphospace may be evidence that this morphological shift is associated with an arboreal lifestyle. Arboreal lizards of the Agamidae family have been shown to have a remarkably similar pattern to what we observe in Iguania; evolving from the edge of the terrestrial morphospace and greatly expanding into a novel morphospace, characterized by longer and more slender skulls<sup>12</sup>. Although the taxonomic scale is much smaller, the similarity of these two studies provides evidence of an adaptive response in head shape during ecological transition into the arboreal niche. However, the precise selective pressure driving this change is not yet known for either group.

After anoles moved into arboreal habitats, we observe that their cranial shape gradually expanded into a greater morphological space than in the prior 100–160 million years of Iguanian evolution<sup>29</sup>. We did not find evidence of a rapid accumulation of diversity (i.e., early burst), which is consistent with analyses by Harmon<sup>42</sup>. To the contrary, we find that the estimated ancestor of *Anolis* was on the edge of morphospace occupied by their relatives, and species subsequently diversified into a novel, and much larger region of morphospace by making relatively large shifts from one shape to another (i.e., long branches). These large shifts may be associated with repeated transition between microhabitats or migration between islands<sup>11,43</sup>. Therefore, we conclude that changes in evolutionary mode following the origin of *Anolis* explains the extensive diversity in *Anolis* head shape.

The genus *Phrynosoma* possesses a unique row of horns adorning its posterior skull. The number and size of horns varies extensively among species. Because of these ornaments, this genus was not included in this study. Although this genus is unique among all squamates, it is unlikely to affect the overall interpretation of Iguanid skull diversification. The face of *Phrynosoma* is short and round, meaning they would still fall on the side of the morphospace with relatives, not anoles. The morphometric branch length leading to *Phrynosoma* would likely be very long (associated with horn evolution) making it a distant outlier to the greater patterns of Iguanid skull diversity. Future research may benefit from the independent comparisons of anterior and posterior skull evolution as these likely reflect distinct evolutionary modules<sup>37</sup>.

*Anolis* is a textbook example of an adaptive radiation and aspects of this group's postcranial morphology have been studied extensively, especially limb and toe pad traits that directly impact how this group interacts with the habitat and are thought to correlate with its adaptive diversification<sup>11,17,22,36,43</sup>. Prior studies have identified that head shape is diverse and has ecomorphological signal<sup>37,38,42</sup>, but knowledge about the adaptive bases of skull shape diversity lags behind that of the postcranium. Given that the vertebrate head is vital to a species' ability to interact with food sources, communicate, or interact with the environment e.g.,<sup>44,45</sup>, understanding the adaptive bases of head diversity should be a priority of the field. Multiple selection pressures are sure to have worked together to shape this complex structure, and further research is necessary to better understand the selection pressures driving head shape in anoles and their relatives.

Our study has shown that anoles possess a unique skull shape compared to their Iguanian relatives. We hypothesize that this shape difference is due to their predominantly arboreal lifestyle. More specifically, we

hypothesize that a longer face is conducive to a wider gape or faster jaw closure, allowing anoles to capture different prey; the evolution of elongate skulls with a gracile face is known to be biomechanically driven<sup>46</sup>. A streamlined skull shape may also lead to a shallower body form, that does not rise off the surface, which could help with crypsis or balance while moving through complex habitats and narrow structures in trees and raised vegetation<sup>47</sup>. The seminal paper on lizard head shape diversity<sup>48</sup> did not mention any trends in habitat use so the degree to which this pattern is observed among different families with arboreal species is still unknown. Additional comparisons between *Anolis*, and other lizard clades that have arboreal representatives may be particularly fruitful for testing the strength and generalizability of these alternative hypotheses.

Our study highlights how expanding our research beyond the most studied clades and traits can improve our understanding of morphological diversification. The methodological approach used here, where a broad sampling of species outside of the known adaptive radiation was undertaken to provide reference to the focal clade, expands our understanding of organismal changes that occur as species move into a novel ecological space. Analyses such as this will provide the most complete understanding of how changes in morphology correlate with changes in the ecology of an expanding species complex.

## Materials and methods

### Sampling

We collected three-dimensional morphological data from 55 species of *Anolis* and 55 related species from the suborder Iguania (Fig. 1; Table S1). The latter is comprised of a subset of members of the suborder Iguania<sup>49</sup>, including representatives from the families Corytophanidae, Liolaemidae, Leiosaurinae, Enyaliinae, Opluridae, Hoplocercidae, Polychrotidae, Phrynosomatidae, Crotaphytidae, Leiocephalidae, Iguanidae and Tropiduridae. Our assumption when designing this sampling strategy is that variation among families is greater than variation within families. Therefore, we predict that this sampling strategy will approximate the maximum diversity in iguanian cranial form. To account for intraspecific variation, we sampled 2–3 adult individuals of each species (except for *Enyalioides laticeps* and *Anolis leachi*, for which we sampled 1 individual because of availability of intact specimens; Table S1; 290 total specimens). Specimens scanned at Loyola University Chicago were adult males. However, not all publically available data included sex information, and therefore the sex of specimens from Morphosource cannot be guaranteed.

*Phrynosoma*, a genus in the family Phrynosomatidae commonly known as the horned lizards, have a unique skull shape when compared to all the other relative species in the sampling (Fig. S2). Because this genus has extreme elaborations to the back of their skull (i.e., horns), we were unable to confidently measure them with the same landmark scheme, so they were not included in our sampling. Other species in the family Phrynosomatidae were included, including members of *Cophosaurus*, *Holbrookia*, *Sceloporus*, *Petersaurus*, *Uma*, *Urosaurus*, and *Uta*.

### Micro computed tomography

Our sampling consisted of publicly available data from MorphoSource<sup>50</sup>; [www.morphosource.org](http://www.morphosource.org); Table S1] and preserved museum specimens, scanned using a Perkin Elmer Quantum FX μCT Imaging System in the Loyola University Chicago Department of Biology. We placed museum specimens (see Table S1) in a plastic bag, to avoid desiccation, and the head was scanned for 57 min with 90 kV and 88 μA. A filter of copper and aluminum was used for all specimens. We recovered voxel sizes ranging from 20 to 144 μm, depending on specimen size. Novel scans are available on MorphoSource ([www.morphosource.org](http://www.morphosource.org)) Project ID: 000606249.

We created scaled skull models from tomographs (in DICOM or TIFF format) using VGSTUDIO MAX (version 3.4.3). From the 3D volumetric rendering a surface determination was performed so that measurement (3D shape) data could be collected from the skulls.

### Morphometrics

We placed 53 landmarks at homologous points of each specimen's cranium (Fig. S6) using the "Point" tool in VGSTUDIO MAX (version 3.4.3). We did not place landmarks on the casque ornamentation (or flange) of species in the family Corytophanidae (see Fig. 1), but instead placed the landmark at the homologous point, found at the most ventral and posterior part of the flange where it is attached to the rest of the skull.

We analyzed landmark data in the R Statistical Environment [version 4.3.1<sup>51</sup>, using functions in the package *geomorph* version 4.0.5<sup>52,53</sup>, unless stated otherwise. The vertebrate skull is bilaterally symmetric. To account for modest variation between the two sides, the raw landmark data was superimposed and oriented with a generalized Procrustes analysis (GPA), using the function "bilat.symmetry", which takes into account object symmetry of the skulls by averaging the landmark placement on the sides of the skulls, accounting for any variation between those sides<sup>54</sup>. The landmark data representing the symmetric component of shape for all specimens were then averaged by species for further analysis. Landmark measurements were taken on the cranium only and results pertain to cranium shape, however lower jaw is included in figures to aid visualization.

### Phylogenetic comparative analyses

Comparative phylogenetic analyses were done in the context of the Tonini et al.<sup>39</sup> fully sampled squamate time-scaled phylogeny comprising 9574 species. We used the first 1000 posterior trees<sup>42</sup>, which were generated from a combined approach of phylogenetic inference from genetic data [from<sup>49</sup> and taxonomic assignment [The Reptile Database; <sup>31</sup> using the Phylogenetic Assembly using Soft Taxonomic Inferences approach [PASTIS;<sup>55</sup>. These trees included all species sampled here, and *Anolis* was monophyletic in all trees. With respect to our sample of 110 species, the placement of 102 was inferred from molecular data (where 8 species of the outgroup sampling were placed by taxonomic assignment). The trees were trimmed to include only the species in our analyses using the function "keep.tip" in the package *phytools* version 1.5.1<sup>49,56</sup>.

## Statistical analyses

The main axes of shape variation in the skulls were evaluated using a principal component analysis (PCA) on the species-averaged landmarks and visualized on the morphospace (Fig. 3). To visualize the evolutionary history of shape variation in this morphospace, one phylogenetic tree was projected into the morphospace using maximum likelihood estimation of internal nodes using the function “gm.prcomp”, producing a phylomorphospace [*sensu* 42]. Since this is for visualization only, it was not necessary to assess the distribution of all 1000 trees. Shape variation associated with each major PC axis was visualized by warping 3D surface meshes to the landmark configuration representing the minima and maxima of each PC axis (equivalent to PC loadings). A specimen close to the mean shape among all specimens in the study was used for visualizing warps (*Anolis krugi*, FMNH 12395, details in Table S1). It was represented by isosurface of bone voxels from the volumetric data created in VG Studio and imported into R, where it was warped to the mean shape of all skulls, using the function “plotRefToTarget”. This mean skull isosurface was then warped to the shape representing the maximum and minimum PC scores of PC1 and PC2 using the function “warpRefMesh”. Differences between the warped meshes were used to analyze the element(s) of shape for which each PC is responsible (Fig. 3). To better tease apart the changes happening in the landmark configuration, thin plate spline warps were also generated (Fig. S3), which better identify the subtle shape changes along PC2.

For each of the 1000 trees, we performed the following statistical analyses in a phylogenetic context. From the distribution of 1000 values of each statistic and p-value, the median value was reported. This approach allows for phylogenetic uncertainty in assessing statistical significance.

Evolutionary allometry was tested using a phylogenetic generalized least squares regression implemented with “procD.pgls”, which assesses statistical significance using a permutation test (1000 iterations). A multivariate regression approach was used to visualize the evolutionary allometry using the regression score approach<sup>57</sup>.

We compared the rate of morphological change in anoles and their relatives using a multivariate approach<sup>58</sup> implemented in the function “compare.evol.rates”. This method estimates the rate of morphological change for each group of species and performs a permutation test randomizing the species between the two groups to test for statistical significance. 1000 random permutations were performed. We evaluated how skull shape disparity changed over time for the entire sampling. We mapped the data and 100 Brownian motion simulations on a disparity through time plot using the function “dtt” in the package geiger<sup>59</sup>. To test whether anoles and their relatives occupy different amounts of morphospace (disparity), we calculated the Procrustes variance (the sum of the diagonal elements of the group covariance matrix divided by the number of observations in the group [e.g.<sup>40</sup>] of each group using the function “morphol.disparity”, which performs a permutational test for significance (1000 iterations).

To evaluate the mode of evolution inferred from the distribution of species in morphospace, we used two complementary statistics following the approach outlined in Sidlauskas<sup>41</sup>. For these the morphospace was restricted to the first 4 PCs totaling just under 75% of the variance (74.9%). The first statistic is the length of morphometric branches, calculated as the Euclidean distance between nodes or terminal bracketing the branch. This analysis informs us about how much morphological change is happening from each node to tip of a branch, where a high value indicates that a lot of morphological change happened as that species diverged from the most recent common ancestor, while a shorter morphometric branch length indicates that the change in shape is more conserved. The second statistic is the lineage density for a group, calculated as the sum of the morphometric branch lengths divided by a measure of disparity (the amount of morphospace occupied). We used Lineage Density 2, which is a more conservative measure that considers the dimensionality of the data. Student's t-tests were implemented with “t.test” to compare between groups the distribution of mean morphometric branch lengths and lineage densities calculated from 1000 trees. These were implemented using R scripts provided by B. Sidlauskas.

## Data availability

The µCT slice data are archived on MorphoSource ([www.morphosource.org](http://www.morphosource.org)) project ID: 000606249 [https://www.morphosource.org/projects/000606249/temporary\\_link/cH8HS99yiWS5iaVnxT9Ez8qy?locale=en](https://www.morphosource.org/projects/000606249/temporary_link/cH8HS99yiWS5iaVnxT9Ez8qy?locale=en). Landmark data and R scripts are archived on Dryad. They can be accessed using this reviewer sharing link: <http://datadryad.org/stash/share/IPETU4oarwFDJmNhzaD2gxVVLVGERNkzyZhPfr9-Q2g>.

Received: 1 April 2024; Accepted: 13 December 2024

Published online: 30 December 2024

## References

1. Gillespie, R. G. et al. Comparing adaptive radiations across space, time, and taxa. *J. Hered.* **111** (1), 1–20 (2020).
2. Schlüter, D. *The Ecology of Adaptive Radiation* (Oxford University Press, 2000).
3. Lack, D. *Darwin's Finches* (Cambridge University Press, 1947).
4. Witter, M. S. & Carr, G. D. Adaptive radiation and genetic differentiation in the hawaiian silversword alliance (compositae: Madiinae). *Evolution* **42** (6), 1278–1287 (1988).
5. Kornfield, I. & Smith, P. F. African cichlid fishes: Model systems for evolutionary biology. *Annu. Rev. Ecol. Syst.* **31** (1), 163–196 (2000).
6. Abzhanov, A. et al. The calmodulin pathway and evolution of elongated beak morphology in Darwin's finches. *Nature*, **442**(7102), (2006).
7. Lamichhaney, S. et al. Evolution of Darwin's finches and their beaks revealed by genome sequencing. *Nature*, **518**, (2015).
8. Salzburger, W. Understanding explosive diversification through cichlid fish genomics. *Nat. Rev. Genet.* **19** (11), 705–717 (2018).
9. Enbody, E. D. et al. Community-wide genome sequencing reveals 30 years of Darwin's finch evolution. *Science* **381**, eadbf6218 (2023).
10. Stroud, J. T. & Losos, J. B. Ecological opportunity and adaptive radiation. *Annu. Rev. Ecol. Evol. Syst.* **47** (1), 507–532 (2016).

11. Burruss, E. D. & Muñoz, M. M. Ecological opportunity from innovation, not islands, drove the anole lizard adaptive radiation. *Syst. Biol.* **71** (1), 93–104 (2021).
12. Gray, J. A., Sherratt, E., Hutchinson, M. N. & Jones, M. E. H. Evolution of cranial shape in a continental-scale evolutionary radiation of Australian lizards. *Evolution* **73** (11), 2216–2229 (2019).
13. Mahler, D. L., Revell, L. J., Glor, R. E. & Losos, J. B. Ecological opportunity and the rate of morphological evolution in the diversification of greater Antillean anoles. *Evolution* **64** (9), 2731–2745 (2010).
14. Miles, D. B., Ricklefs, R. E. & Losos, J. B. How exceptional are the classic adaptive radiations of passerine birds? *Proceedings of the National Academy of Sciences*, **120**(35), e1813976120. (2023).
15. Poe, S. et al. A phylogenetic, biogeographic, and taxonomic study of all extant species of *Anolis* (Squamata; Iguanidae). *Syst. Biol.* **66** (5), 663–697 (2017).
16. Stroud, J. T. & Losos, J. B. Bridging the process-pattern divide to understand the origins and early stages of adaptive radiation: A review of approaches with insights from studies of *Anolis* lizards. *J. Hered.* **111** (1), 33–42 (2020).
17. Losos, J. B. The Evolution of Form and Function: Morphology and Locomotor Performance in West. *Indian Anolis Lizards Evol.* **44** (5), 1189–1203 (1990).
18. Grant, P. R. & Grant, R. B. Evolution of character displacement in Darwin's finches. *Science* **313**, 224–226 (2006).
19. Albertson, R. C., Streelman, J. T. & Kocher, T. D. Directional selection has shaped the oral jaws of Lake Malawi cichlid fishes. *PNAS* **100** (9), 5252–5257 (2003).
20. Hedges, S. A. & Arnولد, M. L. Spurring plant diversification: Are floral nectar spurs a key innovation? *Proc. Royal Soc. B: Biol. Sci.* **262**, 343–348 (1995).
21. Hunter, J. P. & Jernvall, J. The hypocone as a key innovation in mammalian evolution. *Proc. Natl. Acad. Sci. U.S.A.* **92** (23), 10718–10722 (1995).
22. Losos, J. B. *Lizards in an Evolutionary Tree: Ecology and Adaptive Radiation of Anoles* (University of California Press, 2009).
23. Poe, S. et al. Comparative evolution of an archetypal adaptive radiation: Innovation and opportunity in *Anolis* lizards. *Am. Nat.* **191** (6), E185–E194 (2018).
24. Patton, A. H. et al. When adaptive radiations collide: Different evolutionary trajectories between and within island and mainland lizard clades. *Proc. Natl. Acad. Sci.* **118** (42), e2024451118 (2021).
25. Miller, A. H. & Stroud, J. T. Novel tests of the key innovation hypothesis: Adhesive toepads in arboreal lizards. *Syst. Biol.* **71** (1), 139–152 (2021).
26. LaRouche, O., Gartner, S. M., Westneat, M. W. & Evans, K. M. Mosaic evolution of the skull in labrid fishes involves differences in both tempo and mode of morphological change. *Syst. Biol.* **72** (2), 419–432 (2023).
27. Slater, G. J. & Friscia, A. R. Hierarchy in adaptive radiation: A case study using the Carnivora (Mammalia). *Evolution* **73** (3), 524–539 (2019).
28. Muñoz, M. M., Frishkoff, L. O., Pruitt, J. & Mahler, D. L. Evolution of a model system: New insights from the study of *Anolis* lizards. *Annu. Rev. Ecol. Evol. Syst.* **54** (1), 475–503 (2023).
29. Pyron, R. A. Novel approaches for phylogenetic inference from morphological data and total-evidence dating in squamate reptiles (Lizards, Snakes, and Amphisbaenians). *Syst. Biol.* **66** (1), 38–56 (2017).
30. Sherratt, E., Gower, D. J., Klingenberg, C. P. & Wilkinson, M. Evolution of cranial shape in caecilians (Amphibia: Gymnophiona). *Evol. Biol.* **41** (4), 528–545 (2014).
31. Uetz, P. et al. The Reptile Database. The Reptile Database. (2023). <http://www.reptile-database.org/>
32. Pincheira-Donoso, D., Bauer, A. M., Meiri, S. & Uetz, P. Global taxonomic diversity of living reptiles. *PLOS ONE*, **8**(3), e59741. (2013).
33. Edwards, D. L., Avila, L. J., Martinez, L., Sites Jr, J. W. & Morando, M. Environmental correlates of phenotypic evolution in ecologically diverse *Liolaemus* lizards. *Ecol. Evol.* **12**(6), e9009. (2022).
34. Pincheira-Donoso, D., Harvey, L. P. & Ruta, M. What defines an adaptive radiation? Macroevolutionary diversification dynamics of an exceptionally species-rich continental lizard radiation. *BMC Evol. Biol.* **15** (1), 153 (2015).
35. Harmon, L. J., Schlute, J. A., Larson, A. & Losos, J. B. Tempo and mode of evolutionary radiation in Iguanian lizards. *Science* **301**, 961–964 (2003).
36. Losos, J. B. & Sinervo, B. The effects of morphology and perch diameter on sprint performance of *Anolis* lizards. *J. Exp. Biol.* **145** (1), 23–30 (1989).
37. Sanger, T. J., Mahler, D. L., Abzhanov, A. & Losos, J. B. Roles for modularity and constraint in the evolution of cranial diversity among *Anolis* lizards: *Anolis* skull shape and modularity. *Evolution* **66** (5), 1525–1542 (2012).
38. Sanger, T. J. et al. Convergent evolution of sexual dimorphism in skull shape using distinct developmental strategies: skull shape dimorphism among *Anolis* lizards. *Evolution* **67** (8), 2180–2193 (2013).
39. Tonini, J. F. R., Beard, K. H., Ferreira, R. B., Walter, J. & Pyron, R. A. Fully-sampled phylogenies of squamates reveal evolutionary patterns in threat status. *Biol. Conserv.* **204**, 23–31 (2016a).
40. Zelditch, M., Swiderski, D. & Sheets, H. D. *Geometric Morphometrics for Biologists: A Primer* (Academic, 2012).
41. Sidlauskas, B. Continuous and arrested morphological diversification in sister clades of characiform fishes: A phylomorphospace approach. *Evolution* **62** (12), 3135–3156 (2008).
42. Harmon, L. J. et al. Early bursts of body size and shape evolution are rare in comparative data. *Evolution* **64** (8), 2385–2396 (2010).
43. Beutell, K. & Losos, J. B. Ecological morphology of Caribbean anoles. *Herpetological Monogr.* **13**, 1–28 (1999).
44. Kraatz, B. & Sherratt, E. Evolutionary morphology of the rabbit skull. *PeerJ* **4**, e2453 (2016).
45. Marcy, A. E., Hadly, E. A., Sherratt, E., Garland, K. & Weisbecker, V. Getting a head in hard soils: Convergent skull evolution and divergent allometric patterns explain shape variation in a highly diverse genus of pocket gophers (*Thomomys*). *BMC Evol. Biol.* **16** (1), 207 (2016).
46. Mitchell, D. R., Sherratt, E. & Weisbecker, V. Facing the facts: Adaptive trade-offs along body size ranges determine mammalian craniofacial scaling. *Biol. Rev.* **99**(2). (2023).
47. Young, J. W. Convergence of arboreal locomotor specialization: morphological and behavioral solutions for movement on narrow and compliant supports. In: (eds Bels, V. L. & Russell, A. P.) *Convergent Evolution. Fascinating Life Sciences*. Springer, Cham. (2023).
48. Stayton, C. T. Morphological evolution of the lizard skull: A geometric morphometrics survey. *J. Morphol.* **263** (1), 47–59 (2005).
49. Pyron, R., Burbrink, F. T. & Wiens, J. A. A phylogeny and revised classification of Squamata, including 4161 species of lizards and snakes. *BMC Evol. Biol.* **13** (1), 93 (2013).
50. Watkins-Colwell, G. et al. The walking dead: Status report, data workflow and best practices of the oVert thematic collections network. *Biodivers. Inform. Sci. Stand.* **2**, e26078 (2018).
51. R Core Team. R: A Language and Environment for Statistical Computing. R Foundation for Statistical Computing. (2023). <https://cloud.r-project.org/> [Computer software].
52. Adams, D. C., Collyer, M. L., Kaliontzopoulou, A. & Baken, E. Geometric Morphometric Analyses of 2D/3D Landmark Data (4.0.6) <https://cran.r-project.org/package=geomorph> (2023). [Computer software].
53. Baken, E., Collyer, M., Kaliontzopoulou, A. & Adams, D. geomorph v4.0 and gmShiny: Enhanced analytics and a new graphical interface for a comprehensive morphometric experience. *Methods Ecol. Evol.* **12** (11), 1–9 (2021).
54. Klingenberg, C. P., Barluenga, M. & Meyer, A. Shape analysis of symmetric structures: quantifying variation among individuals and asymmetry. *Evolution* **56** (10), 1909–1920 (2002).

55. Thomas, G. H. et al. PASTIS: An R package to facilitate phylogenetic assembly with soft taxonomic inferences. *Methods Ecol. Evol.* **4** (11), 1011–1017 (2013).
56. Revell, L. J. phyttools: An R package for phylogenetic comparative biology (and other things). *Methods in Ecology and Evolution*, **3**, 217–223. (2012).
57. Drake, A. G. & Klingenberg, C. P. The pace of morphological change: Historical transformation of skull shape in St Bernard dogs. *Proc. Royal Soc. B: Biol. Sci.* **275** (1630), 71–76 (2008).
58. Adams, D. C. Quantifying and comparing phylogenetic evolutionary rates for shape and other high-dimensional phenotypic data. *Syst. Biol.* **63** (2), 166–177 (2014).
59. Harmon, L. J., Wein, J. T., Brock, C. D., Glor, R. E. & Challenger, W. GEIGER: Investigating evolutionary radiations. *Bioinformatics* **24** (1), 129–131 (2008).
60. Tonini, J. F. R., Beard, K. H., Ferreira, R. B., Walter, J. & Pyron, R. A. Data from: Fully-sampled phylogenies of squamates reveal evolutionary patterns in threat status. Dryad: (2016). <https://doi.org/10.5061/dryad.db005> [dataset].

## Acknowledgements

The authors thank Loyola University Chicago Department of Biology for access to scanning and computational resources and general support. Martin Berg and Joseph Milanovich provided guidance on research design. The authors also thank the following institutions for providing access to data used in this study. The files were downloaded from [www.MorphoSource.org](http://www.MorphoSource.org) (Duke University): American Museum of Natural History. Cleveland Museum of Natural History. Field Museum of Natural History. Special thanks to Joshua Mata for assistance with borrowing from the herpetology collections. Florida Museum of Natural History, University of FloridaNatural History Museum of Los Angeles CountyMuseum of Comparative Zoology, Harvard University Museum of Vertebrate Zoology, UC Berkeley Smithsonian Institution, National Museum of Natural HistoryTexas A&M University Biodiversity Research and Teaching Collections (TCWC)University of KansasYale Peabody Museum.

## Author contributions

KS, ES, TJS, conceptualized the manuscript, performed the research, prepared figures, and wrote the manuscript. All authors edited and reviewed the manuscript before submission.

## Funding

National Science Foundation (NSF) IOS award #1942250 (TJS and KBS). Australian Research Council (ARC) Future Fellowship award FT190100803 (ES).

## Competing interests

The authors declare no competing interests.

## Additional information

**Supplementary Information** The online version contains supplementary material available at <https://doi.org/10.1038/s41598-024-83404-5>.

**Correspondence** and requests for materials should be addressed to T.J.S.

**Reprints and permissions information** is available at [www.nature.com/reprints](http://www.nature.com/reprints).

**Publisher's note** Springer Nature remains neutral with regard to jurisdictional claims in published maps and institutional affiliations.

**Open Access** This article is licensed under a Creative Commons Attribution-NonCommercial-NoDerivatives 4.0 International License, which permits any non-commercial use, sharing, distribution and reproduction in any medium or format, as long as you give appropriate credit to the original author(s) and the source, provide a link to the Creative Commons licence, and indicate if you modified the licensed material. You do not have permission under this licence to share adapted material derived from this article or parts of it. The images or other third party material in this article are included in the article's Creative Commons licence, unless indicated otherwise in a credit line to the material. If material is not included in the article's Creative Commons licence and your intended use is not permitted by statutory regulation or exceeds the permitted use, you will need to obtain permission directly from the copyright holder. To view a copy of this licence, visit <http://creativecommons.org/licenses/by-nc-nd/4.0/>.

© The Author(s) 2024